# Spectral Shifts and Dissociation Dynamics of Acetone in the Presence of an External Electric Field

Xinyao Liu[1,2], M. Umar Majeed[1,2], Boyuan Han[1,2], Hassnain Khalil[1,2] and Yuzhu Liu[1,2,*]

[1]*State Key Laboratory Cultivation Base of Atmospheric Optoelectronic Detection and Information Fusion, Nanjing University of Information Science & Technology, Nanjing 210044, China*

[2]*Jiangsu International Joint Laboratory on Meteorological Photonics and Optoelectronic Detection, Jiangsu Collaborative Innovation Center on Atmospheric Environment and Equipment Technology (CICAEET), Nanjing University of Information Science & Technology, Nanjing 210044, China*

**Abstract:** Acetone, a typical volatile organic compound (VOC), poses significant environmental and health risks due to its high reactivity and contribution to the photochemical smog formation. The effects of an external electric field (EEF) ranging from 0 to 30.854 V·nm$^{-1}$ on the physical and chemical properties of acetone were investigated by density functional theory (DFT) using the B3LYP/6-311+g(2d,2p) basis set. The results demonstrate that the C=O bond in acetone elongates and the total moment increases as the EEF increases, enhancing molecular polarization. Although the total energy of acetone decreases with increasing EEF, the change is primarily due to the dipole-field interaction, and does not necessarily indicate improved thermodynamic stability. The infrared (IR), Raman, and UV-Vis spectra exhibit redshifts, indicating a reduction in excitation energy. Single-point energy scans confirm that the C=O bond weakens, with dissociation predicted at 52.785 V·nm$^{-1}$.

**Keywords:** DFT, EEF, dissociation, IR spectrum, Raman spectrum.

## 1. INTRODUCTION

Acetone, dimethyl ketone ($C_3H_6O$), is a simple saturated ketone. It is a common volatile organic compound (VOC) that is widely used in industrial processes and as a solvent [1-3]. While acetone has important applications in various fields, its presence in the atmosphere poses environmental and health risks [4-8]. As a major VOC, acetone contributes to photochemical smog formation and affects atmospheric oxidants and ozone levels, making its degradation an important topic of research. Traditional methods for acetone removal, such as adsorption and photocatalysis, have been studied extensively [9-12]. However, these methods are often limited by efficiency or require significant energy input.

More recently, applying different external electric fields to the molecules has been proposed to affect the reactivity and dissociation of their properties [13, 14]. The effects of EEFs on VOC dissociation, particularly acetone, remain insufficiently understood. Therefore, applying an EEF to acetone could potentially be an efficient method [15, 16].

In this manuscript, an EEF ranging from 0 to 30.852V·nm$^{-1}$ was applied for the calculations using the DFT method based on the B3LYP/6-311+g(2d,2p) basis set to examine the physical properties of acetone accurately. When the EEF changes, the Raman and infrared (IR) absorption spectra of acetone change. The potential energy surface obtained through single-point energy scanning was used to analyze the dissociation process of acetone molecules. Additionally, the energy gap of acetone provides insight into the dissociation process of acetone under the EEF.

## 2. EXPERIMENTAL TECHNIQUES AND THEORETICAL MODELS

### 2.1. Computational Method and Theoretical Model

The system's Hamiltonian (*H*) under consideration describes the interaction between the acetone molecule and the EEF, as represented in Eq. (1):

$$H = H_0 + H_{\text{int}} \tag{1}$$

Here, $H_0$ represents the Hamiltonian of the molecular system in the absence of an EEF, describing the intrinsic property of the acetone molecule, including its kinetic energy and potential energy due to bonding forces and other molecular properties like rotational and vibrational modes. $H_{int}$ represents the interaction system and how the molecular system interacts with the EEF.

The dipole approximation assumes a uniform electric field across the molecule, valid for weak fields where the molecule is much smaller than the distance over which the field varies, and higher-order effects (like quadrupole or octupole moments) can be neglected. In such a dipole approximation, $H_{int}$ is expressed by Eq. (2):

$$H_{\text{int}} = -\mu \cdot F \tag{2}$$

*Address correspondence to this author at the State Key Laboratory Cultivation Base of Atmospheric Optoelectronic Detection and Information Fusion, Nanjing University of Information Science & Technology, Nanjing 210044, China; E-mail: yuzhu.liu@nuist.edu.cn

Received on 10-09-2025 Accepted on 24-10-2025 Published on 29-10-2025

E-ISSN: 2311-8741/25

where $\mu$ represents the dipole moment of acetone, and $F$ is the EEF applied to the system[17]. The dipole moment of acetone results in the asymmetric electron distribution, and the C=O bond dipole is mainly dominant in $\mu$. The negative sign indicates that the energy of the molecular system drops when the dipole aligns with the EEF, and such alignment happens because the EEF acts as a force on the dipole. The EEF in this study ranges from 0 to 30.852V·nm$^{-1}$, whereas 1a.u. = 5.14225 × 10$^{11}$V·m$^{-1}$.

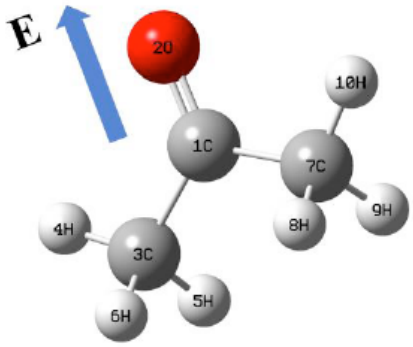


**Figure 1:** The ground state molecular structure of acetone, with the blue arrow showing the direction of the EEF.

In this study, Gaussian 09 Revision A.1 serves as the primary computational tool for calculating molecular structures and plays a significant role in studying the complex changes in molecules' physical and chemical properties under the influence of EEF[18-20]. Considering that the changes in acetone properties are mainly attributed to variations in the carbonyl group C=O, the EEF is applied along the Z-axis. The field direction can be adjusted using the “field” keyword in Gaussian 09 Revision A.1[20]. As shown in Figure **1**, the C=O bond of acetone is aligned along the Z-axis in the Cartesian coordinate system, with the blue arrow indicating the direction of the EEF.

### 2.2. Schematic Illustration of the Experimental Setup for Detecting Acetone Molecules

In this paper, an experiment is designed to collect Raman spectra of the acetone molecule, which means the Raman setup represents an actual experiment. The schematic diagram of the experimental setup is shown in Figure **2**, which includes a single-mode semiconductor laser and a Raman spectrometer. Initially, a 532nm laser beam emitted by the laser is directed onto the acetone sample. The Raman scattering signal from acetone is collected by the signal probe and transmitted through the Raman spectrometer to a computer. Finally, the experimentally collected Raman spectra are compared with the Raman spectra of acetone molecules optimized based on the basis set B3LYP/6-311+g(2d,2p), mainly by comparing their characteristic peaks, to validate the accuracy of this computational method.

## 3. RESULTS AND DISCUSSION

### 3.1. Geometrical Configuration of the Ground State

In this manuscript, various computational methods are employed to improve the consistency between the acetone model and the experimental data. The geometric structure of acetone was calculated and compared under different methods and basis sets in the absence of an EEF. The optimal method was selected based on the smallest root mean square error (RMSE) of the C=O bond and C-C bond lengths compared to the experimental value [31]. The comparison results are shown in Table **1**. And the smallest RMSE indicates that the DFT method based on the B3LYP/6-311+g(2d,2p) basis set results in the experimental values, making it the most suitable choice for the following calculations.

### 3.2. Physical characteristics under an applied EEF

The molecular structure of acetone consists of carbon, oxygen, and hydrogen atoms bonded among C=O, C-C, and C-H bonds. Considering the significance of the 1C=2O and 1C-3C bonds in the structure and the crucial influence made by dipole moment and total energy on the structural changes of acetone, this study investigates the impact of EEF on

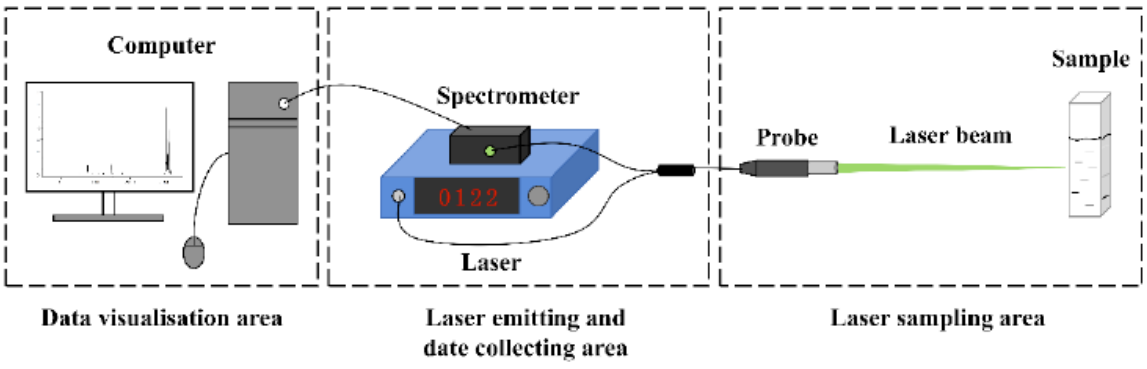


**Figure 2:** Schematic overview of the experimental arrangement.

**Table 1: The Calculation of Different Basis Sets on the Bond Length of Acetone**

| Methods | $R_{1C-2O}(10^{-10}m)$ | $R_{1C-3C}(10^{-10}m)$ | RMSE |
|---|---|---|---|
| B3LYP/6-311+(d) | 1.21250 | 1.51748 | 0.0019367 |
| B3LYP/6-311+g(d,p) | 1.21178 | 1.51665 | 0.0016212 |
| B3PW91/6-311+g(d,p) | 1.20974 | 1.51164 | 0.0033751 |
| B3PW91/6-311+g(2d,2p) | 1.20888 | 1.51019 | 0.0050497 |
| **B3LYP/6-311+g(2d,2p)** | **1.21067** | **1.51488** | **0.0004623** |
| Experimental values | 1.21095 | 1.51523 | |

the acetone molecule characteristics. As illustrated in Table **2**, the results demonstrate a correlation between the change in total energy, bond lengths, and the dipole moment of acetone. Figure **3** illustrates the relationship between increasing EEF strength and the elongation of the C=O (1C=2O) bond, indicating that this bond weakens and becomes more prone to rupture. Conversely, the 1C-3C bond exhibits a slight decrease in length, suggesting a gradual bond compression. This phenomenon can be attributed to the enhanced Coulomb force within the C=O bond, which generates a greater internal electric field force compared to the applied EEF, counteracting its influence [19]. Under the increasing EEF, the weakening of the C=O bond slightly increases the total energy, the more significant role is played by the more stable energy from the dipole-field interaction, resulting in a decrease in the total energy.

According to the data shown in Figure **4**, the total energy of the acetone molecule consistently decreases, indicating an increase in its stability. This phenomenon originates from the interaction between the molecular dipole and the EEF, governed by the system's interaction Hamiltonian ($H_{in}$), which leads to a stabilization of the system energy. It is important to emphasize that this energy reduction reflects a stabilization effect of the molecule within the EEF and does not indicate a better molecular stability. In fact, the strength of the C=O bond demonstrates a decrease in the structural stability of the molecule. Furthermore, the molecule's dipole moment exhibits an evident upward trend, which generally indicates an increase in charge polarization due to the EEF, and eventually a reduction in the total energy of the system. The polarization effect and the changes in bond length demonstrate that while the total energy of the system decreased under the EEF, the chemical reactivity of the molecule is actually enhanced.

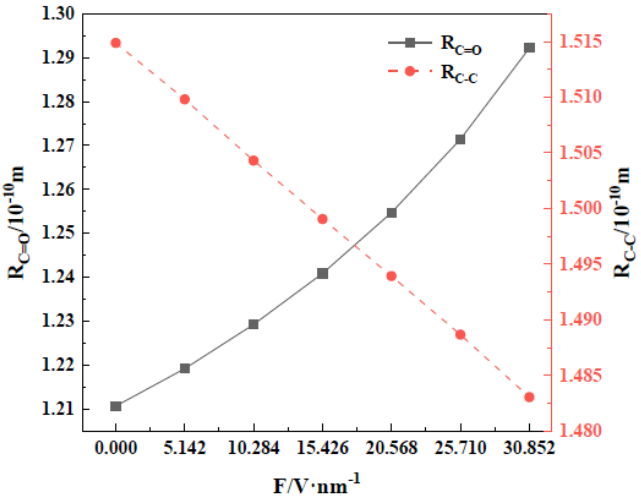


**Figure 3:** The change of $R_{C=O}$ and $R_{C-C}$ under different EEFs (from 0 to 30.852 V·nm$^{-1}$).

**Table 2: The Bond Lengths, Dipole Moment, and Total Energy of the Acetone**

| F(V·nm$^{-1}$) | $R_{1C-2O}(10^{-10}m)$ | $R_{1C-3C}(10^{-10}m)$ | Dipole Moment (Debye) | Total Energy (Hartree) |
|---|---|---|---|---|
| 0 | 1.21067 | 1.51488 | 3.1011 | -193.226 |
| 5.142 | 1.21918 | 1.50981 | 4.3527 | -193.240 |
| 10.284 | 1.22925 | 1.50430 | 5.6338 | -193.260 |
| 15.426 | 1.24088 | 1.49905 | 6.9671 | -193.285 |
| 20.568 | 1.25470 | 1.49393 | 8.388 | -193.315 |
| 25.710 | 1.27142 | 1.48866 | 9.9437 | -193.351 |
| 30.852 | 1.29217 | 1.48304 | 11.7146 | -193.393 |

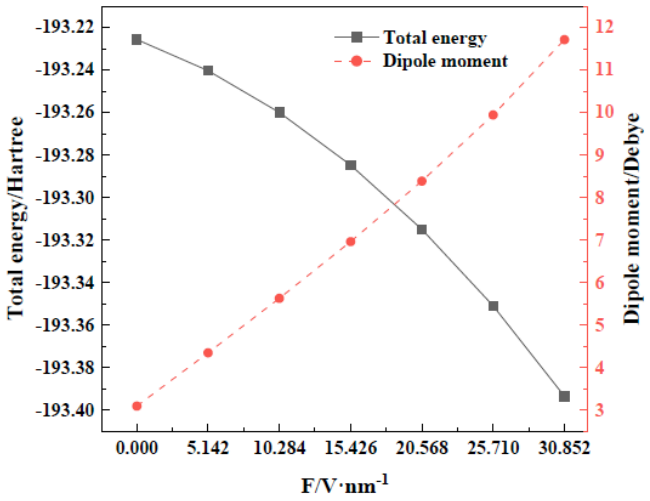


**Figure 4:** The change of dipole moment and total energy under different EEFs (0 to 30.852 V·nm$^{-1}$).

### 3.3. Impact of an EEF on the Energy Gap and Frontier Orbital's Energy Level

In this study, the changes of the highest occupied molecular orbital (HOMO), the lowest unoccupied molecular orbital (LUMO), and the energy gap ($E_G$) of acetone molecules under various EEF (from 0 to 30.852 V·nm$^{-1}$) were computed using the B3LYP/6-311+g(2d,2p) computational method. The LUMO represents the lowest energy molecular orbital that is unoccupied by electrons, and its energy ($E_L$) indicates the molecule's electron acceptance capacity, whereas a lower $E_L$ corresponds to a better tendency for the acetone to acquire electrons[16]. Conversely, the HOMO represents the highest-energy molecular orbital that is occupied by electrons, and a higher HOMO energy ($E_H$) suggests a greater likelihood of electron donation. Furthermore, the $E_G$ indicates the energy difference between $E_H$ and $E_L$, and the calculation method with unit conversion is provided in Eq. (3). A smaller $E_G$ implies easier energy absorption, facilitating electronic transitions from the HOMO to the LUMO, thereby making the molecule more susceptible to excitation or chemical reactions.

$$E_G = (E_L - E_H) \times 27.2114eV \quad (3)$$

The results of the acetone molecules under different EEF are shown in Figure **5**. As the EEF increases, $E_L$ showed a continuous decreasing trend, initially at a slow rate, while then accelerating. Simultaneously, $E_H$ decreases steadily. Moreover, $E_G$ increases with the EEF up to 10.284 V·nm$^{-1}$, after which it decreases sharply. This decline may be attributed to the rapid decrease in the $E_L$ when the EEF ranges from 10.284 V·nm$^{-1}$ to 30.852 V·nm$^{-1}$. This can be explained as a direct consequence of the EEF and the inherent electron density distribution of the frontier orbitals. When the EEF is aligned with the C=O bond, with its positive end oriented towards the electronegative oxygen atom, it preferentially stabilizes orbitals with significant electron density on oxygen. While the LUMO is primarily decided by the carbonyl group and is therefore more strongly stabilized by the EEF, leading to the observed rapid drop in E. Figure **5** also presents the diagrams of the corresponding frontier orbitals of the acetone molecule under different EEFs, where the arrow represents the direction of the EEF. The gap initially shows a slight increase for weaker fields but decreases sharply as the EEF strengthens beyond 10.284 V·nm$^{-1}$, where the intense stabilization of the LUMO takes the lead. A reduced $E_G$ signifies a lower energy requirement for electronic excitations from HOMO to LUMO, thereby enhancing the molecule's chemical reactivity.

The orbital visualization in Figure **5** proves that under a strong EEF of 30.852 V·nm$^{-1}$, the electron density of both frontier orbitals obviously changed and separated along the EEF. This charge redistribution confirms that the EEF directly disturbs the molecular potential and facilitates electronic transitions. The change of electronic and geometric structure above contributes to the molecular destabilization and supports the predicted dissociation behavior at higher EEF.

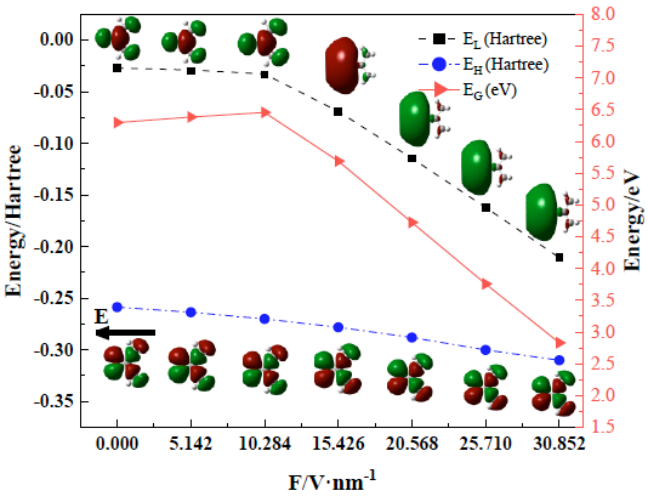


**Figure 5:** The change of $E_H$, $E_L$, and $E_G$ of acetone under different EEFs (0 to 30.852 V·nm$^{-1}$).

### 3.4. Dissociation of the Acetone Molecules under Different EEFs

The B3LYP/6-311+g(2d,2p) computational method was used to study the dissociation process of acetone molecules under various EEF. The single point energy of the C=O bond in acetone was calculated for bond lengths ranging from 0.8×10$^{-10}$m to 2.6×10$^{-10}$m of 0.1×10$^{-10}$m. The results of these calculations are shown in Figure **6**.

As the bond length increases, the single-point potential energy of the C=O bond initially decreases sharply before increasing gradually, as shown in Figure **6**. The rise in potential energy after reaching its minimum suggests that the molecule has not yet dissociated. As EEF ranges from 0 to 30.852 V·nm$^{-1}$, the scanning potential energy decreases progressively. When EEF reaches a certain value, the C=O bond may break, leading to the dissociation of acetone molecules. The potential barrier is the difference between the minimum energy corresponding to the most stable bond length and the maximum energy of the unstable point[19]. As EEF increases, both the dissociation energy and potential barrier decrease gradually.

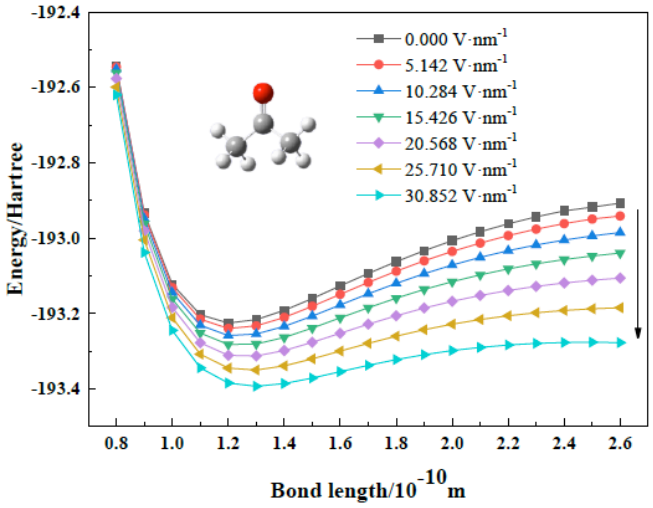


**Figure 6:** The potential energy of the acetone under different EEFs (0 to 30.852 V·nm$^{-1}$).

A linear fitting analysis of the potential energy barrier across various electric field strengths (EEF) is illustrated in Figure **7**, which reveals a high correlation coefficient ($R^2$ = 0.99944). This robust linear correlation substantiates a direct proportional relationship between the energy barrier and the EEF. The computational results indicate that acetone molecules will dissociate at an EEF strength of approximately 52.785 V·nm$^{-1}$, suggesting that acetone molecules can be dissociated via the C=O chemical bond. While this field strength is substantial, it corresponds with the principles of field-induced bond breaking and finds relevance in ccertain environments.

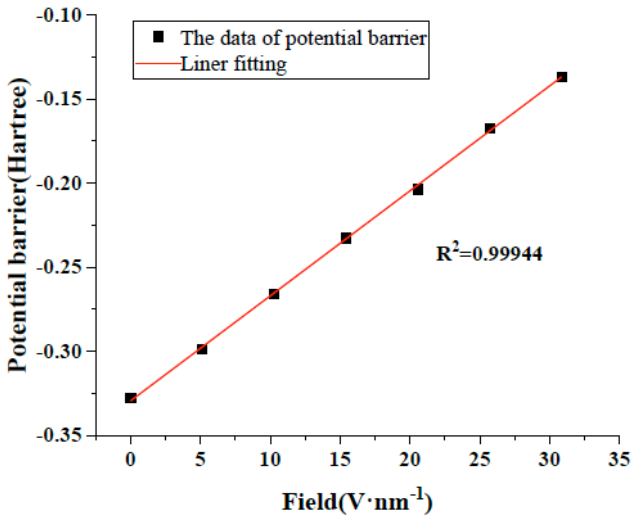


**Figure 7**: The linear fit curve of the potential barrier under the EEFs.

### 3.5. Changes of the IR spectrum and Raman spectrum under EEF

The B3LYP/6-311+g(2d,2p) computational method was employed to study the infrared absorption spectrum of the optimized acetone molecule under the influence of EEF. The infrared absorption spectrum reveals molecular vibrations and functional group absorption peaks. As shown in Figure **8**, the acetone molecule without EEF exhibits 24 vibrational modes, including various vibrational modes of the C=O, C-C, and C-H bonds. This study primarily focuses on three significant peaks associated with the stretching vibration of the C=O bond, and the strongest peak corresponds to 1779.24 cm$^{-1}$. Figure **9** compares the experimental spectra from NIST and the calculated infrared spectra under the B3LYP/6-311+g(2d,2p) for the optimized structure of the acetone molecule in the range of 0~3800 cm$^{-1}$ under zero EEF [21]. The experimental values correspond well with the calculated values, and the intensity distribution of the three characteristic peaks of C=O also conforms to theoretical expectations, validating the reliability of the B3LYP/6-311+g(2d,2p) computational method within the framework of DFT calculations under zero electric field conditions.

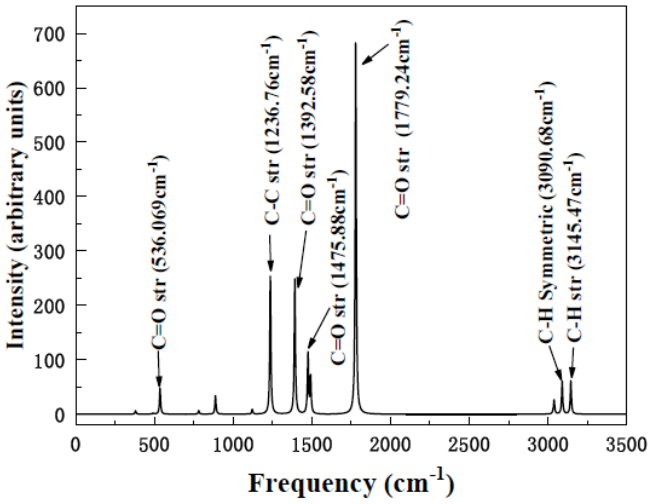


**Figure 8:** IR spectrum of the acetone (0 to 3500 cm$^{-1}$) under zero EEF.

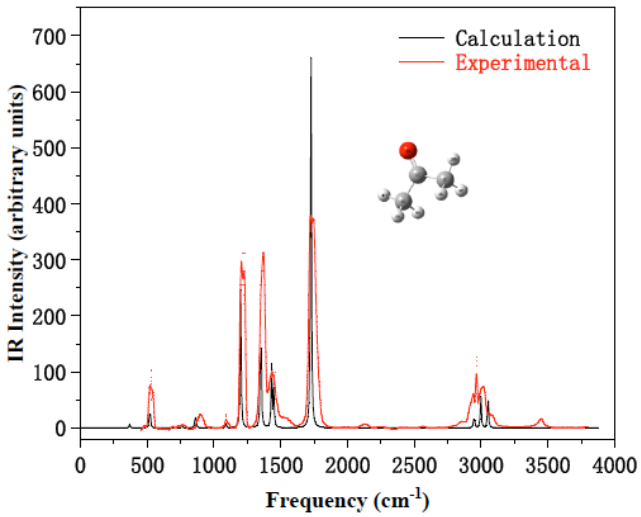


**Figure 9:** The calculated and experimental results of the IR spectrum (0 to 3500 $cm^{-1}$) under the zero EEF.

Figure **10** shows the effect of the EEF increasing from 0 to 30.852 $V \cdot nm^{-1}$ on the infrared spectrum of acetone molecules, and the stretching vibration changes of C=O bonds in the range of 1200 $cm^{-1}$ to 1870 $cm^{-1}$ are the main focus. With the increase of EEF, the strongest absorption peak corresponding to the symmetric stretching vibration of the C=O bond has a red shift from 1779.24 $cm^{-1}$ to 1500.3 $cm^{-1}$. The peak intensity initially increased and then decreased, and when the EEF increased from 25.710 to 30.852 $V \cdot nm^{-1}$, the peak intensity decreased sharply. At the same time, the absorption peak of C=O stretching at 1392.58 $cm^{-1}$ shifted to 1302.5 $cm^{-1}$, the peak value continued to increase, and finally became the most important absorption peak of C=O symmetric vibration at 30.852 $V \cdot nm^{-1}$, indicating that this vibration was the most significant at this time. Additionally, the infrared peak at 1475.88 $cm^{-1}$ undergoes a redshift to 1419.64 $cm^{-1}$, while its vibration intensity increases steadily. The change of the C=O bond under the action of EEF can be explained by the Stark effect, which can be seen by Y. Wang *et al*. [22, 23]. When the absorption peak of C=O is redshifted, less energy is required for this vibration, and at stronger EEFs, the molecules are more unstable and even easily dissociate.

Figure **11** compares the experimental and calculated Raman values for the optimized structure of the acetone molecule in the range of 0 to 3500 $cm^{-1}$ under zero EEF. The experimental values are collected by experimental arrangement and are in good agreement with the calculated values, which indicate that the B3LYP/6-311+g(2d,2p) computational method under DFT calculation selected in this study, under zero EEF, is suitable. Figure **12** shows the change of the Raman spectrum of acetone in the range of 2880 to 3190 $cm^{-1}$ due to the increase of the EEF from 0 to 30.852 $V \cdot nm^{-1}$. Raman spectroscopy is a type of scattering spectrum that supplements infrared spectroscopy [30], and each peak represents the vibration of a particular molecular bond. Furthermore, as the EEF increases, the strongest peak of the Raman spectroscopy undergoes a redshift. This shift indicates a significant change in the molecular vibration frequency. This variation in peak intensities shows that some vibrational modes are enhanced while others are suppressed. This redshift can be explained by the reduction of the $E_G$, and the strong EEF stabilizes the LUMO more than the HOMO, narrowing the $E_G$ and consequently decreasing the energy required for electronic transitions, and this exactly is the electronic Stark effect. This behavior shows that under different EEFs, the C-H bond becomes unstable.

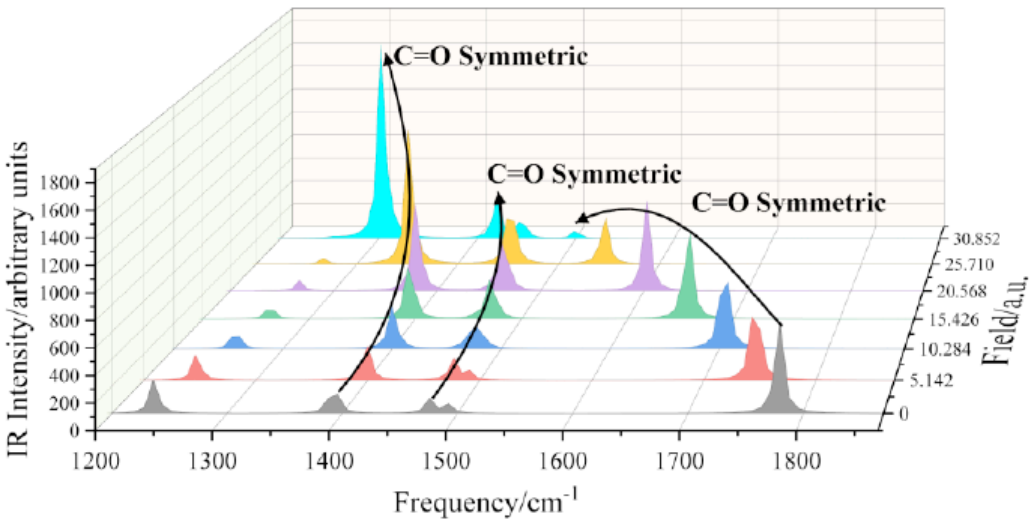


**Figure 10:** The change of the IR spectrum of the acetone from 1200 to 1870 $cm^{-1}$ under different EEFs (from 0 to 30.852 $V \cdot nm^{-1}$).

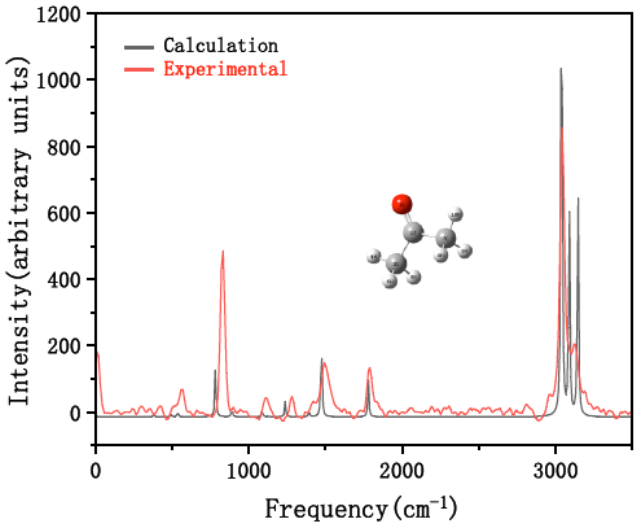


**Figure 11:** The calculated and experimental results of the Raman spectrum (0 to 3500 $cm^{-1}$) without EEF.

### 3.6. Changes of the UV-Vis Epsilon Spectrum under EEF

In this study, the TD-DFT method with the B3LYP/6-311+g(2d,2p) basis set was used to simulate the UV-Vis absorption spectra of acetone molecules under different EEFs (including 0, 15.426V·$nm^{-1}$, 20.568V ·$nm^{-1}$, and 25.710V ·$nm^{-1}$). The results of UV-Vis spectra of acetone molecules in the range of 0-800 nm under different EEFs are shown in Figure **13**. The main focus is on the change of the strongest absorption peak of C=O. The UV-Vis absorption spectrum of acetone exhibits a typical molecular Stark effect [24]. On the one hand, when the EEF changes from 0 to 25.710 V·$nm^{-1}$, the most significant absorption peak shifts from 204.56 nm to 504.5 nm, and the peak intensity gradually decreases. On the other hand, with the increase of EEF, the second significant peak also undergoes a redshift from 176.31 nm to 276.64 nm, and the peak value increases first and then decreases. This significant redshift is since the $H_{int}$ term lowering the LUMO energy level much more than the HOMO energy, narrowing the energy gap $E_G$ and leading to an increase in the wavelength [25]. These results indicate that when the EEF increases, there are two different types of energy required for C=O vibration, and the final trend is that with the increase of the EEF, the energy needed for the C=O bond decreases, which confirms the previously mentioned view that acetone molecules are unstable under strong EEF. At the same time, a new broad and strong absorption band (from 500nm to 600nm) appears at higher EEF due to the field-induced charge transfer states with large transition dipole moments. Furthermore, the overall absorption intensity increases with the EEF strength, which can be attributed to enhanced electronic polarization and greater transition dipole moments. The results demonstrate that the EEF has a significant effect on the energy levels of the acetone molecule and also on its optical properties.

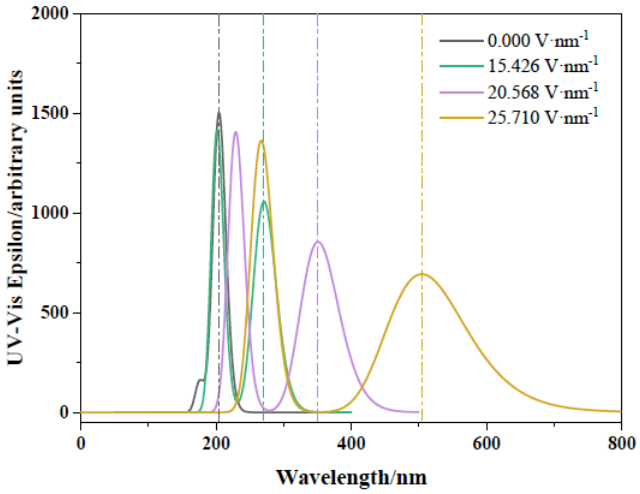


**Figure 13:** The changes of the UV-Vis absorption spectrum of acetone under different EEFs (0.000, 25.710V·$nm^{-1}$).

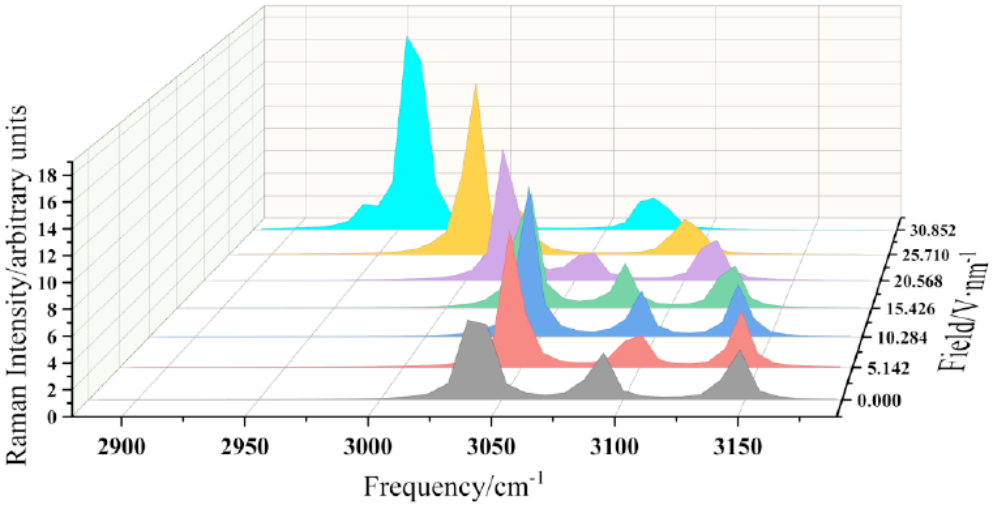


**Figure 12:** The change of Raman spectrum of the acetone (2880 to 3190 $cm^{-1}$) under different EEFs (from 0 to 30.852 V·$nm^{-1}$).

## CONCLUSION

In summary, the acetone molecule was investigated using DFT (B3LYP/6-311+g(2d,2p)) under EEFs (0 to 30.852V·nm$^{-1}$). Structural optimization revealed that increasing the EEF lengthened the C=O bond and shortened the C-C bond due to redistribution, leading to molecule destabilization. The dipole moment increased linearly with EEF, reflecting enhanced charge polarization, while the decreasing total energy indicated improved molecular stability. Frontier molecular orbital analysis showed reduced energy gaps ($E_G$, $E_L$, $E_H$) at higher EEFs (≥10.284 V·nm$^{-1}$), suggesting increased chemical reactivity. Single-point energy scans showed a lower dissociation energy for the C=O bond under EEF, and the linear correlation between the energy barrier and the EEF is high ($R^2$=0.99944), with bond dissociation occurring around 52.785 V·nm$^{-1}$. Spectroscopic studies under EEF revealed a red shift in C=O and C-H bond vibrational peaks, altered peak intensities, and reduced excitation energy in UV-Vis spectra, facilitating electron transitions. These results confirm that EEFs significantly influence the physicochemical properties of acetone and provide a theoretical basis for electric field-assisted degradation strategies. The observed effects provide a solid theoretical foundation for developing electric field-assisted degradation strategies for acetone and similar volatile organic compounds, potentially enabling more efficient catalytic processes or plasma-based treatment technologies for environmental remediation.

## ACKNOWLEDGMENTS

This work was supported by the National Natural Science Foundation of China (Nos. 62481540172, 62375136).

## DECLARATION OF COMPLETING INTEREST

The author declares that they have no known competing financial interests or personal relationships that could have appeared to influence the work reported in this paper.

## DATA AVAILABILITY

The data supporting the findings of this study are not publicly available upon publication, as there is no appropriate repository for data in this field. However, the data can be made available upon reasonable request from the authors.

## REFERENCES

[1] J. M. Zhang *et al*., "Synthesis of isopropyl acetate by acetone method and its reaction mechanism," Chemical Engineering Research & Design, vol. 174, pp. 386-393, Oct 2021. https://doi.org/10.1016/j.cherd.2021.08.003

[2] A. Mehaney and Ahmed, II, "Acetone sensor based 1D defective phononic crystal as a highly sensitive biosensor application," Optical and Quantum Electronics, vol. 53, no. 2, Feb 2021, Art no. 97. https://doi.org/10.1007/s11082-021-02737-x

[3] M. Ginovyan, M. Petrosyan, and A. Trchounian, "Antimicrobial activity of some plant materials used in Armenian traditional medicine," Bmc Complementary and Alternative Medicine, vol. 17, Jan 2017, Art no. 50. https://doi.org/10.1186/s12906-017-1573-y

[4] H. M. Bi, Y. Liu, F. Y. You, X. Q. Chai, P. T. Xie, and J. P. Hu, "Theoretical Studies on the Reaction Mechanism of Photocatalytic Degradation of Acetone," Asian Journal of Chemistry, vol. 24, no. 4, pp. 1668-1670, 12/14 2011.

[5] H. Y. Zuo, Y. Li, and Y. Z. Liao, "Europium Ionic Liquid Grafted Covalent Organic Framework with Dual Luminescence Emissions as Sensitive and Selective Acetone Sensor," Acs Applied Materials & Interfaces, vol. 11, no. 42, pp. 39201-39208, Oct 2019. https://doi.org/10.1021/acsami.9b14795

[6] L. Wang *et al*., "Properties-enhanced gas sensor based on Cu-doped tellurene monolayer to detect acetone molecule: a first-principles study," Molecular Physics, vol. 119, no. 7, Apr 2021, Art no. e1864490. https://doi.org/10.1080/00268976.2020.1864490

[7] A. Amann *et al*., "The human volatilome: volatile organic compounds (VOCs) in exhaled breath, skin emanations, urine, feces and saliva," Journal of Breath Research, vol. 8, no. 3, Sep 2014, Art no. 034001. https://doi.org/10.1088/1752-7155/8/3/034001

[8] Q. A. Drmosh, I. O. Alade, M. Qamar, and S. Akbar, "Zinc Oxide-Based Acetone Gas Sensors for Breath Analysis: A Review," Chemistry-an Asian Journal, vol. 16, no. 12, pp. 1519-1538, Jun 2021. https://doi.org/10.1002/asia.202100303

[9] K. Zhou *et al*., "Experimental and DFT study on the adsorption of VOCs on activated carbon/metal oxides composites," Chemical Engineering Journal, vol. 372, pp. 1122-1133, Sep 2019. https://doi.org/10.1016/j.cej.2019.04.218

[10] W. Xiang *et al*., "Enhanced adsorption performance and governing mechanisms of ball-milled biochar for the removal of volatile organic compounds (VOCs)," Chemical Engineering Journal, vol. 385, Apr 2020, Art no. 123842. https://doi.org/10.1016/j.cej.2019.123842

[11] K. Zhang *et al*., "Morphology-Controlled SmMn2O5 Nanocatalysts for Improved Acetone Degradation," ACS Applied Nano Materials, vol. 6, no. 13, pp. 12114-12123, 2023/07/14 2023. https://doi.org/10.1021/acsanm.3c01862

[12] H. H. Liao, H. Y. Xu, X. W. Zhang, W. X. Dai, and Z. Z. Zhang, "Stable bidentate coordination sulfated TiO2 for highly durable photocatalytic degradation of gaseous acetone," Applied Catalysis a-General, vol. 657, May 2023, Art no. 119158. https://doi.org/10.1016/j.apcata.2023.119158

[13] Z. Liu, J. Y. Luo, Y. Peng, Y. H. Yang, Z. Zeng, and L. Q. Li, "Preparation of Phosphorus-containing Porous Carbon by Direct Carbonization for Acetone Adsorption," Colloids and Surfaces a-Physicochemical and Engineering Aspects, vol. 606, Dec 2020, Art no. 125431. https://doi.org/10.1016/j.colsurfa.2020.125431

[14] H. Lin *et al*., "The studies on the physical and dissociation properties of chlorobenzene under external electric fields," Journal of Theoretical and Computational Chemistry, vol. 17, no. 04, p. 1850029, 2018. https://doi.org/10.1142/S0219633618500293

[15] Z. Y. Zhou, X. Y. Zhang, Y. Z. Liu, and B. Abulimiti, "Study on physical properties of ethylbenzene under external electric field," Computational and Theoretical Chemistry, vol. 1207, Jan 2022, Art no. 113533. https://doi.org/10.1016/j.comptc.2021.113533

[16] C. Yu, Z. M. Sun, Z. Y. Zhou, H. Z. Gao, and Y. Z. Liu, "Study on the dissociation properties and spectra of chlorodifluoromethane under an external electric field,"

Computational and Theoretical Chemistry, vol. 1225, Jul 2023, Art no. 114164. https://doi.org/10.1016/j.comptc.2023.114164

[17] T. Stuyver, D. Danovich, J. Joy, and S. Shaik, "External electric field effects on chemical structure and reactivity," Wiley Interdisciplinary Reviews-Computational Molecular Science, vol. 10, no. 2, Mar 2020, Art no. e1438. https://doi.org/10.1002/wcms.1438

[18] J. Tang, N. Aizezi, C. Yu, and Y. Liu, "Study on the dissociation properties and spectra of iodobenzene under external electric field," Physica Scripta, vol. 99, no. 3, p. 035401, 2024. https://doi.org/10.1088/1402-4896/ad20bc

[19] B. Y. Han, J. Feng, N. Aizezi, and Y. Z. Liu, "Study on the physical and chemical properties of dimethyl sulfoxide under the external electric field," Physica Scripta, vol. 98, no. 11, Nov 2023, Art no. 115011. https://doi.org/10.1088/1402-4896/acfce8

[20] M. J. Frisch, G.W.T., H. B. Schlegel, G. E. Scuseria, M. A. Robb, J. R. Cheeseman, G. Scalmani, V. Barone, B. Mennucci, G. A. Petersson, H. Nakatsuji, M. Caricato, X. Li, H. P. Hratchian, A. F. Izmaylov, J. Bloino, G. Zheng, J. L. Sonnenberg, M. Hada, M. Ehara, K. Toyota, R. Fukuda, J. Hasegawa, M. Ishida, T. Nakajima, Y. Honda, O. Kitao, H. Nakai, T. Vreven, J. A. Montgomery, Jr., J. E. Peralta, F. Ogliaro, M. Bearpark, J. J. Heyd, E. Brothers, K. N. Kudin, V. N. Staroverov, R. Kobayashi, J. Normand, K. Raghavachari, A. Rendell, J. C. Burant, S. S. Iyengar, J. Tomasi, M. Cossi, N. Rega, J. M. Millam, M. Klene, J. E. Knox, J. B. Cross, V. Bakken, C. Adamo, J. Jaramillo, R. Gomperts, R. E. Stratmann, O. Yazyev, A. J. Austin, R. Cammi, C. Pomelli, J. W. Ochterski, R. L. Martin, K. Morokuma, V. G. Zakrzewski, G. A. Voth, P. Salvador, J. J. Dannenberg, S. Dapprich, A. D. Daniels, Ö. Farkas, J. B. Foresman, J. V. Ortiz, J. Cioslowski, and D. J. Fox, Gaussian 09 (Gaussian, Inc., Wallingford CT, 2009).

[21] e. D. E. Gray, "American Institute of Physics Handbook," p. Third Edition, McGraw Hill:New York 1972.

[22] Y. Wang, X. Lin, M. Wang, and X. Li, "Properties of CF3SO2F under the influence of external electric field: A DFT study," Results in Physics, vol. 45, p. 106248, 2023/02/01/ 2023. https://doi.org/10.1016/j.rinp.2023.106248

[23] S. Sowlati-Hashjin and C. F. Matta, "The chemical bond in external electric fields: Energies, geometries, and vibrational Stark shifts of diatomic molecules," The Journal of chemical physics, vol. 139, no. 14, 2013. https://doi.org/10.1063/1.4820487

[24] N. D. Gurav, S. P. Gejji, and R. K. Pathak, "Electronic Stark effect for a single molecule: Theoretical UV response," Computational and Theoretical Chemistry, vol. 1138, pp. 23-38, 2018/08/15/ 2018. https://doi.org/10.1016/j.comptc.2018.05.018

[25] E. T. J. Nibbering and T. Elsaesser, "Ultrafast Vibrational Dynamics of Hydrogen Bonds in the Condensed Phase," Chemical Reviews, vol. 104, no. 4, pp. 1887-1914, 2004/04/01 2004. https://doi.org/10.1021/cr020694p

https://doi.org/10.12974/2311-8741.2025.13.02